

Cite this: *New J. Chem.*, 2011, **35**, 649–662

www.rsc.org/njc

PAPER

Asymmetrically substituted distyrylbenzenes and their polar crystal structures†

Alain Collas,^a Roeland De Borger,^a Tatyana Amanova,^a
 Christophe M. L. Vande Velde,^{†a} Jan K. Baeke,^a Roger Dommissie,^b
 Christian Van Alsenoy^a and Frank Blockhuys^{*a}

Received (in Victoria, Australia) 24th September 2010, Accepted 17th December 2010

DOI: 10.1039/c0nj00732c

The synthesis of twelve asymmetric donor–acceptor distyrylbenzene derivatives with either one nitrile group or one, two or three nitro groups as electron acceptors, and one, two or three methoxy groups as electron donors is reported. Peak potentials obtained from cyclic voltammetry were combined with experimental UV/Vis data and molecular dipole moments obtained from quantum chemical calculations, yielding insight into the influence of the positions of the substituents on the electronic structure and charge distribution of this as yet unexplored class of organic semiconductors. The supramolecular structures of five of these compounds have been studied using single-crystal X-ray diffraction to monitor the influence of the positions of donor and acceptor groups on the organisation of the molecules in the solid state, and three crystal structures have been identified in which the molecular dipoles do not organize themselves in a centrosymmetric lattice. Analysis of the dipoles in the unit cell yields further insight into the possible non-linear optical properties of these three polar structures.

1. Introduction

Organic semiconductors are materials that enjoy considerable interest these days mainly because of the convenient and easy way in which their molecular structures and hence their properties can be tuned to a specific application. This is in stark contrast to the present-day CMOS (Complementary Metal Oxide Semiconductor) technology where such tuning is virtually impossible. Switching from polymeric to oligomeric organic materials is a worthwhile undertaking for the numerous opto-electronic applications for which these new compounds are used, as has been discussed in depth by Müllen and Wegner¹ and Segura and Martín.² The most important reason for making this transition is the fact that it is far easier to produce, purify and structurally characterise oligomers than polymers, as they are monodisperse materials. For these reasons oligomers have been extensively used as model compounds for polymers but it is far more rewarding to study

the properties of these oligomeric organic semiconductor materials for their own sake.

The structure and electronic properties of one particular class of organic semiconductors, *i.e.*, 1,4-distyrylbenzene (DSB) and its derivatives, which are oligomers of poly(*p*-phenylene vinylene), have already been extensively studied,^{3–19} indicating the usefulness of the 1,4-distyrylbenzene structure as a template for materials with interesting electro-optical properties. So far, though, these investigations have focused almost exclusively on symmetrical derivatives, even though a number of possible applications of these materials, such as non-linear optics (NLO) and non-volatile organic memories, require materials with large dipole moments which can be found only in asymmetrical systems. The most convenient way of achieving this is by introducing electron-donating on one and electron-accepting substituents on the other side of the distyrylbenzene scaffold, thus creating conjugated asymmetrical push–pull systems which exhibit the desired large molecular dipoles. Since the synthetic pathways towards distyrylbenzenes (traditionally the Wittig reaction) allow for a wide variety of substituents to be introduced at various positions on the backbone, these oligomers have the potential to generate a large number of suitable materials for these applications. [Note that a number of asymmetric DSBs have been known for some time (see below), but these have remained uncharacterised until now, apart from a single compound bearing fluorine and *tert*-butyl substituents (CSD refcode²⁰ REFKUI)¹¹ of which only the crystal structure was reported.]

^a Department of Chemistry, University of Antwerp, Universiteitsplein 1, B-2610 Antwerp, Belgium.
 E-mail: frank.blockhuys@ua.ac.be; Fax: +32 3 820 23 10

^b Department of Chemistry, University of Antwerp, Groenenborgerlaan 171, B-2020 Antwerpen, Belgium

† Electronic supplementary information (ESI) available. CCDC reference numbers 760975 (**5b-1**), 760976 (**5b-2**), 760977 (**5c**) and 760979 (**5i**). For ESI and crystallographic data in CIF or other electronic format see DOI: 10.1039/c0nj00732c

‡ Current address: Karel de Grote University College, Department of Applied Engineering, Salesianenlaan 30, B-2660 Antwerp, Belgium.

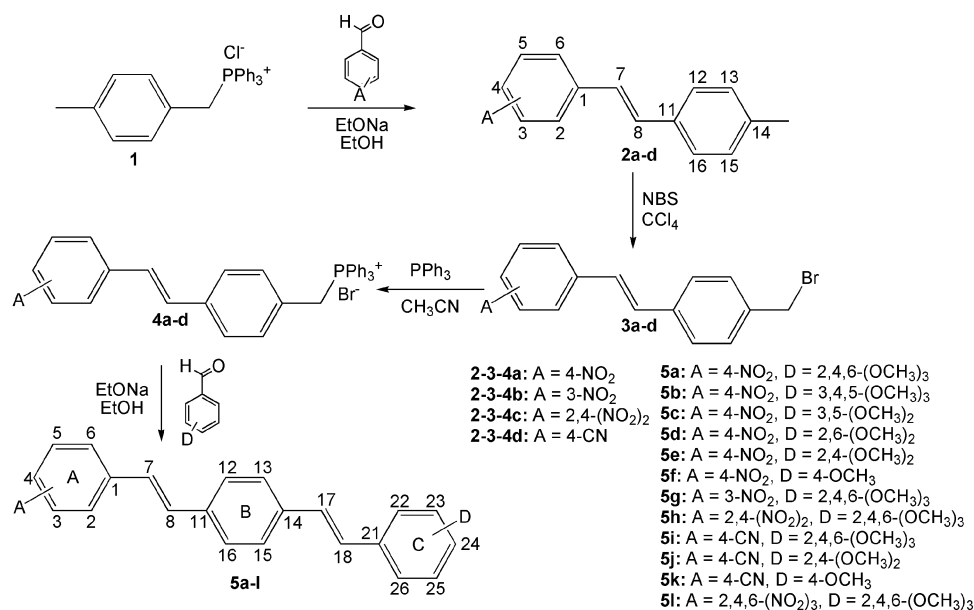


Fig. 1 Synthetic pathway to and structural formulas and numbering scheme of oligomers **5a-1**. Note that **5l** was prepared *via* a different route; see text for details.

Yet, the fact that applications of organic semiconductors generally involve the solid state implies that, apart from the molecular properties, also the properties of the supramolecular structure are of great importance. Indeed, if, for example, the crystal structure is centrosymmetric, the molecular dipoles of asymmetric oligomers are cancelled out by the centre of symmetry in the crystal, thus nullifying the carefully tuned molecular properties generated by the substitution pattern. Since it is still impossible to predict, let alone to control, the space group in which a compound will crystallize, an empirical approach in which the preparation of new materials is followed by the analysis of the supramolecular structure, remains the only option when assessing the applicability of a compound.

In this paper the synthesis and characterisation of twelve new asymmetrical “donor–acceptor” (DA) distyrylbenzenes, containing (one) nitrile or (one, two or three) nitro groups as electron-accepting and (one, two or three) methoxy groups as electron-donating substituents, are reported; the structures of these twelve oligomers (**5a-1**) are presented in Fig. 1. Various combinations of these substituents were used in order to investigate the influence of the number and position of the functionalities on the electronic and (supra)molecular structures of the compounds. The new compounds’ electronic properties were examined using UV/Vis spectroscopy, cyclic voltammetry (CV) and quantum chemical calculations using Density Functional Theory (DFT), and we present the first systematic study of the solid-state structures of asymmetric DSBs, determined using single-crystal X-ray diffraction (XRD).

2. Results and discussion

2.1 Syntheses

The synthetic pathway for the preparation of **5a-k** and the numbering schemes of the compounds are shown in Fig. 1. Triphenyl(4-methylbenzyl)phosphonium chloride

(**1**),²¹ *E*-1-(4-methylphenyl)-2-(4-nitrophenyl)ethene (**2a**),²² *E*-1-(4-methylphenyl)-2-(3-nitrophenyl)ethene (**2b**),²³ *E*-1-(4-methylphenyl)-2-(4-cyanophenyl)ethene (**2d**),¹⁸ *E*-1-(4-bromomethylphenyl)-2-(4-nitrophenyl)ethene (**3a**),¹⁰ *E*-1-(4-bromomethylphenyl)-2-(2,4-dinitrophenyl)ethene (**3c**),²⁴ *E*-1-(4-bromomethylphenyl)-2-(4-cyanophenyl)ethene (**3d**),¹⁸ *E*-triphenyl[4-(2-(4-nitrophenyl)ethenyl)benzyl]phosphonium bromide (**4a**),^{10,24} *E*-triphenyl[4-(2-(4-cyanophenyl)ethenyl)benzyl]phosphonium bromide (**4d**),²⁴ *E,E*-1-[2-(4-nitrophenyl)ethenyl]-4-[2-(2,4,6-trimethoxyphenyl)ethenyl]benzene (**5a**),^{10,24} *E,E*-1-[2-(4-nitrophenyl)ethenyl]-4-[2-(2,4-dimethoxyphenyl)ethenyl]benzene (**5e**),²⁴ *E,E*-1-[2-(4-nitrophenyl)ethenyl]-4-[2-(4-methoxyphenyl)ethenyl]benzene (**5f**)²⁴ and *E,E*-1-[2-(2,4-dinitrophenyl)ethenyl]-4-[2-(2,4,6-trimethoxyphenyl)ethenyl]benzene (**5h**)²⁴ were prepared as previously reported. All benzaldehydes used in the Wittig reactions are commercially available, with the exception of 2,4,6-trinitrobenzaldehyde (**7**) which was prepared²⁵ from 2,4,6-trinitrotoluene (**6**).²⁶ Consequently, **5l** was obtained *via* an adjusted method allowing **7** to be used in the final step: one equivalent of 2,4,6-trimethoxybenzaldehyde reacted with 1,4-bis(triphenylphosphoniummethyl)benzene dibromide, yielding *E*-triphenyl[4-(2-(2,4,6-trimethoxyphenyl)ethenyl)benzyl]phosphonium bromide (**8**), which was condensed in a Wittig reaction with 2,4,6-trinitrobenzaldehyde (**7**), yielding **5l**.

2.2 Molecular properties

2.2.1 Calculated structures. Geometries of the isolated molecules were optimized in their *anti* conformation, in which the two ethenyl spacers are oriented in opposite directions with respect to the central phenyl ring. The resulting structures present no surprises as all but three of the twelve compounds are planar (*C_s* symmetry). In compound **5b**, the methoxy group in the 4-position points out of the plane of the peripheral benzene ring. Compounds **5h** and **5l** have nitro and dinitro substitution in the 2- and 2,6-positions of the acceptor ring,

Table 1 Calculated dipole moments μ (in D) and ionization potentials IP (in eV), experimental peak potentials E_{pa} (in mV vs. Fc/Fc⁺), experimental UV/Vis absorption maxima λ_{max} (in nm) and logarithms of the extinction coefficient ϵ (in $\text{l mol}^{-1} \text{cm}^{-1}$) of compounds **5a–5l**. The values in parentheses in the second column represent the calculated dipole moments (in D) of the molecules in their solid-state geometries. See text for details

	μ	IP	E_{pa}	λ_{max}	$\log \epsilon$
5a	12.20	4.96	456	415	4.70
5b	6.32 (6.19) ^a	5.35	702	197	4.61
5c	5.79 (9.91)	5.47	938	390	4.74
5d	10.54	5.17	715	393	4.21
5e	10.87 (8.71)	5.11	581	408	4.55
5f	9.01	5.30	742	400	4.50
5g	10.36	4.88	479	379	4.63
5h	13.61	5.11	527	449	4.46
5i	11.33	4.90	463	390	4.69
5j	9.71	5.08	582	383	4.15
5k	8.25	5.24	742	376	4.74
5l	12.41	5.19	—	502	4.09

^a For **5b-1**.

respectively, and due to the steric hindrance caused by these nitro groups, the molecules deviate from planarity: the C2–C1–C7–C8 torsion angles are 22.1° and 32.6° for **5h** and **5l**, respectively. These nitro groups are themselves twisted out of the plane of the acceptor ring by 23.5° for the *ortho*-nitro group of **5h**, and 26.2° and 56.7° for those in **5l**, whereas the nitro groups in the *para* position remain in the plane of the ring.

2.2.2 Calculated dipole moments. Considering that the semiconductor applications of these materials mentioned in the Introduction require compounds with large dipole moments, the calculated dipole moments were analyzed in order to investigate the influence of the nature and position of the substituents on their values, which are given in Table 1. The dipole moments of the two related series **5a/5e/5f** (4-nitro substitution) and **5i/5j/5k** (4-cyano substitution) indicate that the dipole moment increases when adding an extra methoxy group by approximately 1.5 D, as expected. The values are also consistently higher for the 4-nitro compounds than for the 4-cyano compounds, indicating that the nitro group is a better electron acceptor. Obviously, 2-, 2,4- and 2,4,6-substitutions (both for acceptor and donor groups) lead to a better charge separation and larger dipole moments than 3- or 3,5-substitution due to the favorable mesomeric conjugation, as can be seen when comparing the values of **5c** and **5e**, **5a** and **5g**, and **5a** and **5b**. The values for 2,6- and 2,4-dimethoxy substitutions (**5d** and **5e**, respectively) are comparable. Although adding one extra nitro group follows the expected trend (**5f** → **5h**), the 2,4,6-trinitro-substituted oligomer (**5l**) shows a decrease in the dipole moment of 1.20 D notwithstanding the additional electron acceptor. The reason for this is most likely the deviation from planarity of the nitro-substituted ring with respect to the rest of the conjugated system and the out-of-plane positions of both *ortho*-nitro groups themselves, leading to a decrease in conjugation.

2.2.3 Electronic properties. The electrochemical characteristics of compounds **5a–5k** were studied using cyclic

voltammetry; the insolubility of **5l** prevented any measurements for this compound. None of the compounds showed a reduction peak and, as a consequence, the formal oxidation potentials could not be determined. Therefore, the anodic peak potentials (E_{pa}) are listed in Table 1. Measurements at different scan rates between 0.03 V s^{-1} and 1 V s^{-1} showed no significant shift of the anodic peak potentials with respect to the oxidation potential of ferrocene, which leads to the conclusion that the absence of the reverse peak is due to a follow-up chemical reaction rather than due to the irreversibility of the system. This has also been observed for a series of self-doping distyrylbenzene derivatives (see ref. 19 and references therein). Therefore, the anodic peak potentials can be used as a measure for the oxidation potential.

When assessing the influence of the electron accepting substituents, a first observation that can be derived from the data in Table 1 is the fact that a cyano group and a nitro group have the same influence on the electronic structure: the peak potentials of the nitro-substituted **5a**, **5e** and **5f** are quite close to those of their cyano-substituted counterparts **5i**, **5j** and **5k**, respectively. This effect is also apparent from the calculated ionization potentials (IP), as similar trends are found. The addition of a nitro group (**5a** → **5h**) increases the peak potential, which can be easily linked to the stabilizing effect of the electron accepting groups on the highest occupied molecular orbital (HOMO), making the oxidation process more difficult. The addition of a third nitro group to the acceptor ring (**5h** → **5l**) can only be inferred from the calculations which do predict a small further increase in the oxidation potential. Moving the single nitro group from the 4-position in **5a** to the 3-position in **5g** has a relatively small effect.

When considering the influence of the number and positions of the electron donating methoxy groups, it is clear that the addition of a methoxy group considerably decreases the peak potential, as seen in the series **5f** → **5e** → **5a** and **5k** → **5j** → **5i**. This can be rationalized when taking into account the destabilization of the HOMO by the increasing number of electron donating groups, leading to an easier oxidation and hence a lower peak potential. As expected, compounds with methoxy substituents in the 3- and 5-positions fare a lot worse (**5b** vs. **5a**, **5c** vs. **5d** and **5e**): the poorer mesomeric and directing properties of these electron donating groups in the *meta*-position(s) are clear. Indeed, when comparing **5c** and **5f**, the peak potential of the latter is much lower even though the former has one extra methoxy group.

As can be seen from the values listed in Table 1, the calculated ionization potentials follow the same trends as the peak potentials. When the E_{pa} values are plotted against these adiabatic ionization potentials, a linear correlation is obtained with $R^2 = 0.88$. This is not a very good correlation *per se* and the lower R^2 value mainly reflects the neglect of solvent effects. In any case, the correlation is better than the one found earlier for a series of symmetrical distyrylbenzene derivatives.⁵

These substituent effects can also be observed in the UV/Vis spectra, as can be seen from Table 1. Removing methoxy groups from the backbone decreases λ_{max} for both the 4-nitro (**5a/5e/5f**) and the 4-cyano (**5i/5j/5k**) series of compounds. Adding nitro groups (**5a** → **5h** → **5l**) increases λ_{max} . Moving

the single nitro group from the 4-position in **5a** to the 3-position in **5g** decreases λ_{\max} .

2.3 Supramolecular structures

Attempts were made to grow single crystals suitable for XRD of all oligomers using various crystallization techniques. However, only for compounds **5a**, **5b**, **5c**, **5e** and **5i** crystals of sufficient size and quality were obtained. The crystal structure of **5a** was reported earlier.¹⁰ Details of the data collection and structural refinement of **5b** (two polymorphs, **5b-1** and **5b-2**), **5c** and **5i** are collected in Table 2. The solid-state structure of **5e** turned out to be dynamically disordered and this disorder was the subject of a separate study;²⁷ the latter paper contains the details of the data collection and structural refinement of **5e**, but a description of the 291 K structure is given below. For all compounds the carbon–hydrogen distances were normalized to 1.083 Å after the refinement and the resulting geometrical parameters were used in the following discussion of the different inter- and intramolecular short contacts involving these hydrogen atoms. The details of these contacts are summarized in Table 3.

2.3.1 E,E-1-[2-(4-Nitrophenyl)ethenyl]-4-[2-(3,4,5-trimethoxyphenyl)ethenyl]benzene (5b). Compound **5b** is crystallized as a mixture of two polymorphs. The first, red polymorph (**5b-1**) crystallizes in the non-centrosymmetric, polar space group $P2_1$ (Table 2). This implies that the molecules do not pair up in a head-to-tail fashion to form centrosymmetric pairs, and that the crystal has a macroscopic polarity. The molecule adopts

the *syn* conformation, with the two ethenyl spacers oriented in the same direction with respect to the central phenyl ring, and is slightly bent along its DA-axis (Fig. 2). The ethenylic link at the donor end of the molecule is disordered, consisting of a 180° pedal-like twist of the double bond (Fig. 3), resulting in about 36% of *anti* conformer. The three benzene rings and two ethenyl spacers in **5b-1** are all virtually co-planar, with dihedral angles between the various rings and spacers of less than about 7° (Table 4).

The packing scheme given in Fig. 2 indicates that the molecules are placed head-to-tail and form ribbons through one CH···O contact between one of the methoxy groups and the nitro group, *i.e.*, C30–H30B···O1. These ribbons are stacked in an anti-parallel fashion by grouping the methoxy-substituted moieties together, connecting successive ribbons by five CH···O and two CH··· π contacts. In one direction these are C40–H40A···O24, C40–H40A···O25 and C50–H50A···Cg(B) [not given in Fig. 2; Cg(B) is the centroid of ring B]. In a second direction these are C15–H15···O24, C16–H16···O1 (not given in Fig. 2), C17–H17···O23 and C30–H30C···Cg(C). Thus, alternating layers of molecules, oriented in an anti-parallel fashion, are formed, creating the typical herringbone structure also found in **5a**.¹⁰

The second, yellow polymorph (**5b-2**) crystallizes in the centrosymmetric space group $P\bar{1}$, with two molecules in the asymmetric unit (Table 2). It transforms into the red polymorph (**5b-1**) upon heating. The two molecules have similar geometries: both are found in the *anti* conformation with a quasi-planar nitro-stilbene moiety, but with a considerably more distorted trimethoxy-stilbene fragment (Table 4).

Table 2 Details of the data collection and structural refinement for **5b** (two polymorphs, **5b-1** and **5b-2**), **5c** and **5i**

	5b-1	5b-2	5c	5i
Formula	C ₂₅ H ₂₃ NO ₅	C ₂₅ H ₂₃ NO ₅	C ₂₆ H ₂₁ NO ₄	C ₂₆ H ₂₃ NO ₃
Formula weight	417.44	417.44	387.42	397.45
Crystal colour	Red	Yellow	Red	Yellow
Crystal size/mm	0.4 × 0.3 × 0.1	0.3 × 0.3 × 0.1	0.3 × 0.3 × 0.3	0.4 × 0.3 × 0.1
Crystal form	Plate	Prism	Prism	Prism
Crystal system	Monoclinic	Triclinic	Monoclinic	Triclinic
Space group	$P2_1$	$P\bar{1}$	$P2_1$	$P\bar{1}$
No. of refl. for cell parameters	25	25	25	25
θ -range (°) for cell measurement	7.48–17.49	7.49–17.67	5.79–15.90	5.55–14.65
$a/\text{Å}$	7.856(2)	10.221(2)	7.219(2)	10.203(3)
$b/\text{Å}$	7.767(2)	15.239(3)	7.402(2)	12.411(2)
$c/\text{Å}$	17.596(6)	15.762(4)	18.163(2)	18.442(2)
α (°)	90.00	117.42(2)	90.00	74.350(10)
β (°)	95.93(2)	92.26(2)	95.29(3)	82.49(3)
γ (°)	90.00	93.52(2)	90.00	70.76(3)
$V/\text{Å}^3$	1067.9(5)	2168.8(8)	966.4(5)	2120.9(7)
Z	2	4	2	4
T	302(2)	300(2)	293(2)	293(2)
$D/\text{Mg m}^{-3}$	1.298	1.278	1.331	1.245
Data collection method	$\omega/2\theta$ scans	$\omega/2\theta$ scans	$\omega/2\theta$ scans	$\omega/2\theta$ scans
θ_{\min} (°)	2.33	1.46	1.13	1.15
θ_{\max} (°)	25.33	25.32	25.33	25.32
Reflections collected	4025	8388	3989	8212
Reflections used in refinement	2105	7906	1919	7741
Parameters used	278	565	262	548
Restraints	4	0	1	7
S.O.F. major conformer (%)	63.9(6)	—	—	85.1(6)
GoOF	1.047	0.975	1.133	1.004
R_w	0.1356	0.1867	0.1752	0.2033
R_u	0.0449	0.0610	0.0594	0.0661
R_{all}	0.1057	0.1854	0.0875	0.1643

Table 3 Details (distances d in Å, angles θ in degrees and symmetry codes) of the short inter- and intramolecular contacts given in the text; the lack of an esd on the parameters is due to the normalisation of the CH distances

Contact	d	θ	Symmetry code
5a			
C17–H17...O22	2.18	117	(Intramolecular)
C18–H18...O26	2.28	102	(Intramolecular)
C2–H2...Cg(C)	2.84	138	$-x, -1/2 + y, 3/2 - z$
C6–H6...Cg(B)	2.59	166	$x, 3/2 - y, 1/2 + z$
C3–H3...O24	2.55	153	$-x, -1/2 + y, 3/2 - z$
C22–H22A...O2	2.45	135	$-x, 1 - y, 2 - z$
C24–H24A...O2	2.63	119	$1 + x, y, -1 + z$
C25–H25...O1	2.20	157	$1 + x, 3/2 - y, -1/2 + z$
C22–H22C...O26	2.70	141	$x, 3/2 - y, -1/2 + z$
5b-1			
C30–H30B...O1	2.37	148	$-1 + x, y, 1 + z$
C40–H40A...O24	2.59	138	$-1 - x, 1/2 + y, 1 - z$
C40–H40A...O25	2.53	156	$-1 - x, 1/2 + y, 1 - z$
C50–H50A...Cg(B)	2.87	159	$-1 + x, y, z$
C15–H15...O24	2.57	160	$-x, 1/2 + y, 1 - z$
C16–H16...O1	2.69	145	$2 - x, 1/2 + y, -z$
C17–H17...O23	2.59	129	$-x, 1/2 + y, 1 - z$
C30–H30C...Cg(C)	2.77	136	$-x, 1/2 + y, 1 - z$
5b-2			
C50–H50C...O924	2.34	163	x, y, z
C6–H6...O24	2.31	173	$1 - x, 1 - y, -z$
C7–H7...O23	2.70	127	$1 - x, 1 - y, -z$
C940–H41B...O23	2.56	171	$1 - x, 2 - y, 1 - z$
C912–H912...O24	2.56	138	$x, -1 + y, z$
C912–H912...O25	2.68	125	$x, -1 + y, z$
C5–H5...O923	2.49	143	$x, -1 + y, -1 + z$
C40–H40B...O923	2.36	164	$1 - x, 2 - y, 1 - z$
C930–H31C...O1	2.71	119	$1 - x, -y, -z$
C926–H926...O2	2.67	148	$-x, -y, -z$
C22–H22...O91	2.70	168	$1 - x, -y, -z$
C30–H30C...O91	2.56	112	$1 - x, -y, -z$
C26–H26...O92	2.57	138	$-x, -y, -z$
5c			
C30–H30B...O1	2.69	115	$2 + x, y, 1 + z$
C30–H30C...O23	2.54	152	$2 - x, -1/2 + y, 1 - z$
C30–H30A...Cg(C)	2.94	120	$2 - x, 1/2 + y, 1 - z$
5e			
C18–H18...O26	2.49	91	(Intramolecular)
C26–H26B...O1	2.49	162	$-1 + x, -y, 1/2 + z$
C24–H24C...O1	2.40	173	$-1 + x, 2 + y, z$
C13–H13...O24	2.70	166	$x, 2 - y, -1/2 + z$
C16–H16...N1	2.53	156	$1 + x, -1 + y, z$
C15–H15...O2	2.40	129	$x, -y, 1/2 + z$
C24–H24B...O26	2.71	138	$x, 1 + y, z$
5i			
C17–H17...O26	2.12	120	(Intramolecular)
C18–H18...O22	2.25	102	(Intramolecular)
C917–H917...O922	2.09	120	(Intramolecular)
C918–H918...O926	2.25	102	(Intramolecular)
C960–H61B...O22	2.60	136	x, y, z
C23–H23...N1	2.41	162	$-1 + x, y, 1 + z$
C95–H95...O26	2.61	132	$1 - x, 1 - y, -z$
C960–H61C...Cg(D)	2.72	133	$1 - x, 1 - y, -z$

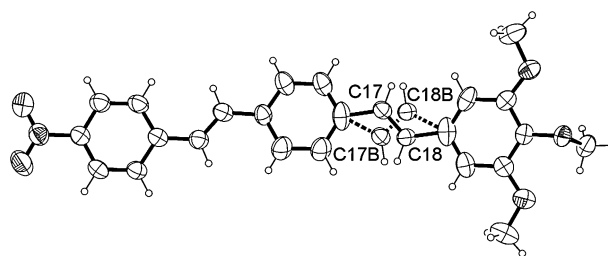


Fig. 3 ORTEP drawing of **5b-1**, showing the disorder of the ethylenic link at the donor end of the molecule. Ellipsoids are drawn at the 30% probability level.

The packing scheme given in Fig. 4 indicates that the two molecules in the asymmetric unit are arranged in a parallel fashion and connected by one CH...O contact [C50–H50C...O924]. Furthermore, molecule 1 is arranged in anti-parallel pairs connected by two CH...O interactions [C6–H6...O24 and C7–H7...O23 (not given in Fig. 4)]. These interactions lead to the 'building block' of four molecules displayed in Fig. 4. These building blocks are stacked through five CH...O interactions (not given in Fig. 4) involving the methoxy groups of molecule 1 [C940–H41B...O23, C912–H912...O24 and C912–H912...O25] and molecule 2 [C5–H5...O923 and C40–H40B...O923] as acceptors. Furthermore, five CH...O contacts (not given in Fig. 4) can be observed involving the nitro groups of molecule 1 [C930–H31C...O1 and C926–H926...O2] and molecule 2 [C22–H22...O91, C30–H30C...O91 and C26–H26...O92]. Clearly, the presence of two molecules in the asymmetric unit leads to a considerably larger number of short contacts. Six additional weaker interactions (five N–O... π and one π ... π) have been compiled in Table S1 of the ESI† (note that when two molecules are present in the asymmetric unit, rings A, B and C of molecule 1 are renamed to D, E and F, respectively, in molecule 2).

2.3.2 E,E-1-[2-(4-Nitrophenyl)ethenyl]-4-[2-(3,5-dimethoxyphenyl)ethenyl]benzene (5c). Compound **5c** crystallizes in the non-centrosymmetric, polar space group $P2_1$ (Table 2). This compound too displays the *anti* conformation and the molecules are nearly planar (Table 4). The packing of **5c** (Fig. 5) shows a large number of similarities with the supramolecular structure of **5b-1**: molecules are organized in

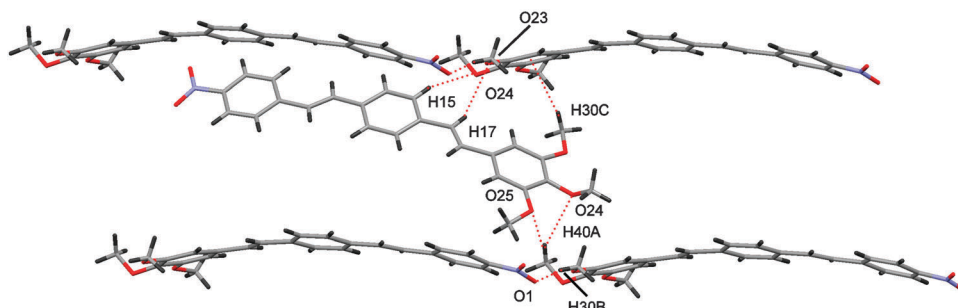


Fig. 2 Packing scheme of **5b-1**, showing the various contacts and the bent form of the molecule. Only the major conformer is shown. See Table 3 for the relevant parameters and symmetry codes.

Table 4 Selected torsion angles (in degrees) for **5b** (two polymorphs, **5b-1** and **5b-2**), **5c**, **5e** and **5i**. For disordered systems, only the values of the major conformer are given. The numbering of Fig. 1 is used

	5b-2			5c	5e	5i	
	5b-1	Molecule 1	Molecule 2			Molecule 1	Molecule 2
C2–C1–C7–C8	–5.6(8)	–4.4(6)	–2.7(7)	–8.6(8)	0.5(8)	14.2(7)	170.0(4)
C1–C7–C8–C11	–176.5(5)	178.0(3)	–176.2(4)	–177.9(5)	–176.8(5)	176.3(4)	179.1(4)
C7–C8–C11–C12	4.8(8)	–2.7(6)	3.6(6)	8.5(8)	–5.9(8)	3.9(7)	178.1(4)
C15–C14–C17–C18	178.2(6)	–20.4(6)	13.3(6)	2.5(8)	–32.2(9)	–179.6(3)	–0.1(6)
C14–C17–C18–C21	173.6(6)	–175.7(3)	–174.8(4)	–177.1(5)	177.6(6)	–172.0(3)	–174.4(3)
C17–C18–C21–C22	–3.7(11)	–19.0(6)	11.7(6)	0.5(8)	–33.4(5)	169.5(3)	6.5(6)

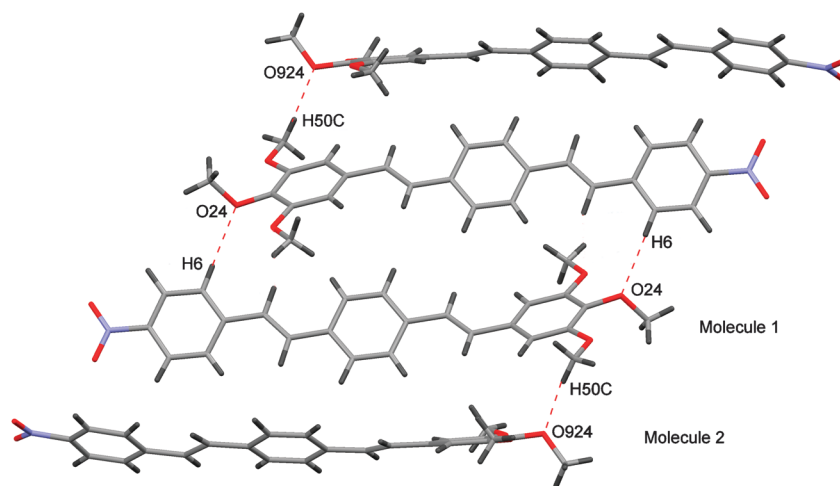


Fig. 4 View of the 'building block' of **5b-2**, showing the relevant CH...O contacts. See Table 3 for the relevant parameters and symmetry codes.

head-to-tail ribbons through a CH...O contact [C30–H30B...O1] and the ribbons are stacked in anti-parallel layers forming a herringbone structure. The methoxy-substituted moieties are connected by one CH...O contact [C30–H30C...O23] and one CH... π contact [C30–H30A...Cg(C), not given in Fig. 5]. Five additional weaker CH... π interactions involving hydrogen atoms on the rings have been compiled in Table S1 (ESI[†]).

2.3.3 E,E-1-[2-(4-Nitrophenyl)ethenyl]-4-[2-(2,4-dimethoxyphenyl)ethenyl]benzene (5e). Compound **5e** crystallizes in the non-centrosymmetric, polar space group *Pc*, again implying macroscopic polarity due to the fact that the molecules do not pair up in a head-to-tail fashion to form centrosymmetric pairs. The molecules display the *anti* conformation. The main feature that is immediately obvious from the packing schemes given in Fig. 6 and 7 is the large deviation of the methoxy-substituted ring C from co-planarity with the rest of the molecule (Table 4). The ethenyl link between rings A and ring B—at the acceptor end of the molecule—is disordered and

the type of disorder is the same as what was observed for **5b-1**. The disorder was fully refined and additional measurements at lower and higher temperatures were performed to study the nature of the disorder, which proved to be dynamic; the full details of this study have been published elsewhere.²⁷ Considering that **5a**,¹⁰ **5b**, **5c** and **5i** (see below) are planar to within about 20°, **5e** is somewhat of an outlier. The reason for this can be found in the intermolecular interactions of the methoxy-substituted ring C (Fig. 6 and 7). An *intramolecular* CH...O contact can be found between the methoxy group positioned *ortho* to the ethenyl link and the hydrogen atoms of that ethenyl link [C18–H18...O26], as expected⁹ (Table 3).

The methoxy group in the 2-position of ring C engages in a CH...O contact with the nitro group of a neighbouring molecule [C26–H26B...O1] as is shown in Fig. 6. The methoxy group in the 4-position is also involved in such a contact [C24–H24C...O1] which is presented in Fig. 7. This same methoxy group simultaneously acts as a hydrogen bond acceptor for two phenyl hydrogen atoms of two different

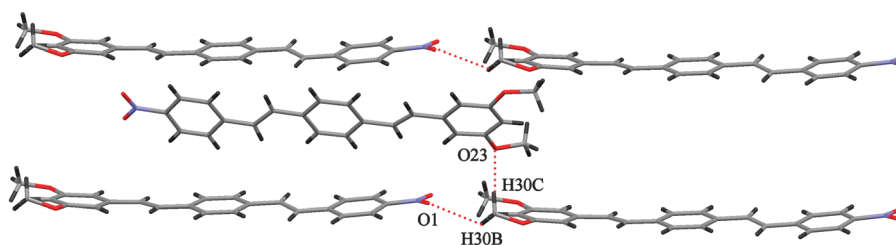


Fig. 5 Packing scheme of **5c**, showing the relevant intermolecular contacts. See Table 3 for the relevant parameters and symmetry codes.

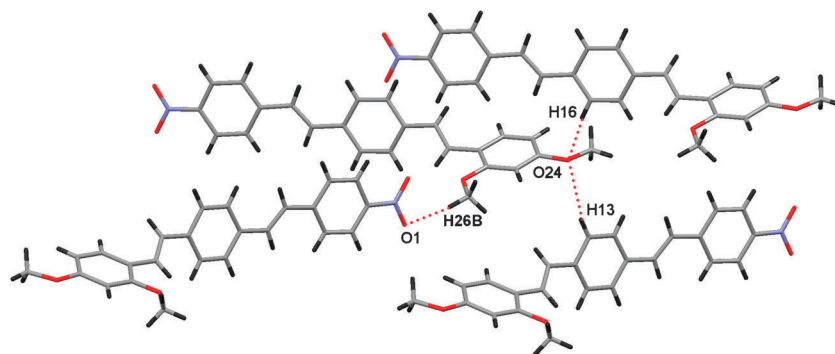


Fig. 6 CH...O contacts involving the methoxy groups in **5e**. Only the major conformer is shown. See Table 3 for the relevant parameters and symmetry codes.

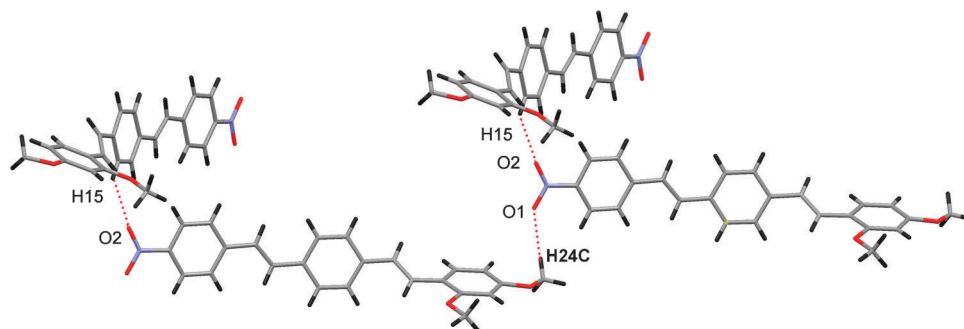


Fig. 7 Ribbons of head-to-tail arranged molecules of **5e** connected by CH...O interactions. The ribbons cross each other at an angle of approximately 50°. Only the major conformer is shown. See Table 3 for the relevant parameters and symmetry codes.

central rings B, in the contacts C13–H13...O24 (the corresponding contact involving the minor conformer has been given in Table S1, ESI†) and C16–H16...O24 (Fig. 6). The overall packing of **5e** consists of ribbons of head-to-tail arranged molecules which cross each other at an angle of approximately 50° (Fig. 7). In between these ribbons one CH...O intermolecular contact between the nitro group and a hydrogen atom of the central ring B can be observed: C15–H15...O2 (Fig. 7, the corresponding contact involving the minor conformer has been given in Table S1, ESI†). A final interaction (not given in Fig. 6 and 7) comprises C24–H24B...O26.

2.3.4 E,E-1-[2-(4-Cyanophenyl)ethenyl]-4-[2-(2,4,6-trimethoxyphenyl)ethenyl]benzene (5i). Compound **5i** crystallizes in the centrosymmetric space group $P\bar{1}$, with two molecules in the asymmetric unit (Table 2). Both molecules display the *syn* conformation around the central ring (Table 4), and are slightly bent along their DA axis (Fig. 8). Molecule 1 displays disorder in the ethenyl link at the acceptor end of the molecule, of the same type as in **5b-1** and **5e**, leading to about 15% of *anti* conformer. The cyano-substituted rings of both molecules are rotated out of the plane of the central ring by no more than 15°. The two independent molecules of **5i** also display four *intramolecular* CH...O contacts: C17–H17...O26, C18–H18...O22, C917–H917...O922 and C918–H918...O926 (Table 3).

The four molecules in the unit cell are arranged with their methoxy-substituted moieties grouped together, connected by CH...O contacts between molecule 1 and molecule 2

[C960–H61B...O22], as shown in Fig. 8. Furthermore, molecule 1 forms an infinite linear chain through the structure, in which the successive molecules are linked by CH...N contacts [C23–H23...N1] (not given in Fig. 8), whereas molecule 2 forms anti-parallel couples due to two additional CH...O [C95–H95...O26] and CH... π [C960–H61C...Cg(D)] contacts (not given in Fig. 8). Four additional weaker interactions (three CH... π involving hydrogen atoms on the rings and one π ... π) have been compiled in Table S1 (ESI†).

2.3.5 E,E-1-[2-(4-Nitrophenyl)ethenyl]-4-[2-(2,4,6-trimethoxyphenyl)ethenyl]benzene (5a). Before comparing the solid-state structures of the five available compounds and six available structures, we will provide a brief description of the crystal structure of **5a**, adapted from ref. 10. Again, the ethenyl spacers are oriented *syn*, as can be seen in Fig. 9. The molecular structure shows a slight deviation from planarity, with angles of 8.28(11)° and 11.03(9)° between rings A and B and between rings B and C, respectively. The overall torsion between rings A and C is 17.92(10)°. There are two *intramolecular* CH...O contacts: C17–H17...O22 and C18–H18...O26 (Table 3).

The molecule crystallizes in the centrosymmetric space group $P2_1/c$, yielding a structure in which the dipoles are lined up between co-facially stacked pairs of molecules related through translation/inversion symmetry. These pairs of molecules form extended double ribbons along the $[-1\ 0\ 1]$ direction. The symmetry equivalent molecules through the glide planes form their own ribbons in the same $[-1\ 0\ 1]$

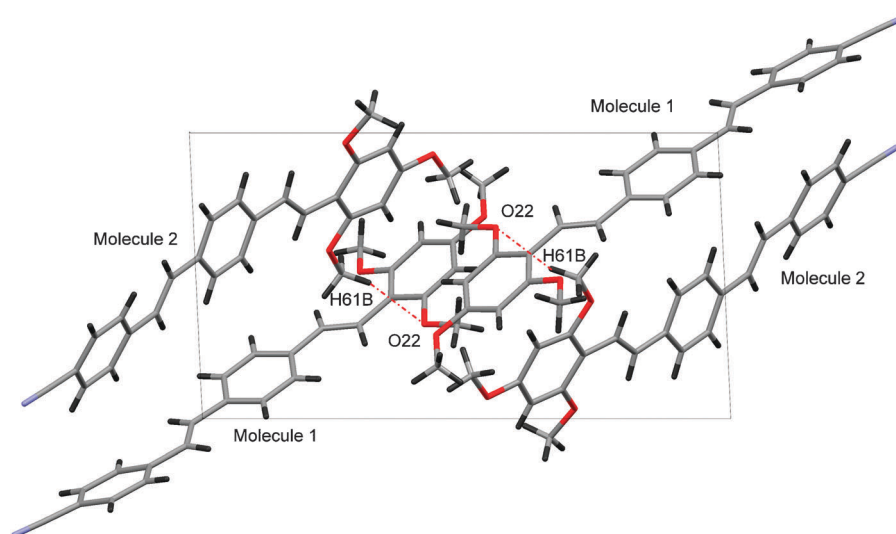


Fig. 8 View along the *b* axis of the four molecules in the unit cell of **5i**, showing the relevant CH...O contacts. Only the major conformer of molecule 1 is shown. See Table 3 for the relevant parameters and symmetry codes.

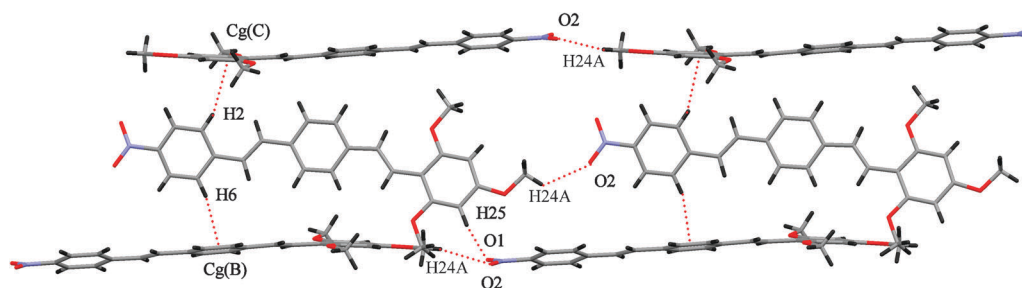


Fig. 9 View of the packing of **5a**, showing the head-to-tail CH...O contacts and the CH... π contacts responsible for the herringbone structure. See Table 3 for the relevant parameters and symmetry codes.

direction. The mutually perpendicular ribbons interact through typical herringbone CH... π contacts originating from the nitro-substituted ring A to rings B and C (Fig. 9): C2–H2...Cg(C) and C6–H6...Cg(B). Between these same molecules, H3 is involved in the contact C3–H3...O24 (not given in Fig. 9). Three other short contacts are weak hydrogen bonds involving the oxygen atoms of the nitro groups: C22–H22A...O2 (not given in Fig. 9), C24–H24A...O2 and C25–H25...O1. The methoxy group in the 2-position also contacts the one in the 6-position of a neighbouring molecule (C22–H22C...O26, not given in Fig. 9). A single N–O... π is given in Table S1 (ESI[†]).

2.3.6 The supramolecular structures of asymmetric distyrylbenzenes. Three of the six compounds and/or polymorphs under investigation crystallize in the *syn* conformation, *i.e.*, **5a**,¹⁰ **5b-1** and **5i**, and this is quite rare for *E,E*-distyrylbenzenes: a CSD search (version 5.30, September 2009 update)²⁰ reveals that only five compounds (CSD refcodes²⁰ GEJTUL,²⁸ GEJVAT,²⁸ PEBRAP,³ QERWUF²⁹ and WEFOZ)¹⁴ show this particular conformation; these are all symmetrically substituted DSBs.

It is clear that the packing of these asymmetric compounds is determined in the first instance by the large molecular dipoles. These are organized in a head-to-tail fashion, creating

infinite strings of likewise oriented molecules. These strings are then stacked in an anti-parallel fashion with respect to each other, with the donor and acceptor moieties placed on top of each other, a packing arrangement which is also present in REFKUI.¹¹ This logically results in *centrosymmetric* crystal structures, which are indeed found for **5a**,¹⁰ **5b-2** and **5i**. Further stabilization of the supramolecular structures is then obtained from intermolecular contacts (Table 3) involving primarily the methoxy groups which create a network of CH...O contacts. Other types of short contacts such as CH... π , CH...N, NO... π and π ... π are observed but more limited in number. However, three of the crystal structures are *not* centrosymmetric: **5b-1** and **5c** crystallize in the non-centrosymmetric, polar space group $P2_1$ and **5e** in the non-centrosymmetric, polar space group Pc . Apparently, in these cases, the dominating effects of the molecular dipoles are overcome and *non-centrosymmetric* space groups are obtained. Strings of dipoles organized in a head-to-tail fashion are still seen, but the combined effects of the intermolecular CH...O and CH... π interactions ultimately outweigh those of the dipoles in the other two directions.

Complementing these *intermolecular* CH...O contacts, *intramolecular* CH...O contacts are found when *ortho*-methoxy substitution with respect to the ethenylic link is present,⁹ as in the structures of **5a**,¹⁰ **5e** and **5i**. These contacts are

undoubtedly the reason why disorder of the ethenyl spacer is not observed at the donor side of the molecules: when *ortho*-methoxy substitution is present the energy barrier for rotation of the double bond is greatly increased.⁷ Note that **5b-1** shows disorder of the ethenyl spacer at the donor side of the molecule but lacks *ortho*-methoxy substitution, and that **5e** and **5i** show disorder of the ethenyl spacer at the acceptor side.

A striking feature is the similarity of the packings of **5b-1** and **5c**. Adding a methoxy group to the 3,5-disubstituted moiety when going from **5c** to **5b-1** apparently does not force the structure to pack in a drastically different way, although the methoxy group in the 4-position is involved in two CH \cdots O contacts. Furthermore, given the fact that the structures are very similar, it seems odd that the major conformer of **5b-1** is *syn* as opposed to **5c** which has an *anti* conformation. This can be rationalized when considering that **5b-1** in the *syn* conformation generates an extra CH \cdots O contact which is absent in its *anti* conformation.

Keeping the possible applications of these compounds in mind and considering that they all require solid states with a macroscopic dipole moment, centrosymmetric structures are *a priori* useless, however excellent the molecular properties of a particular compound may be. Therefore, it is clear that when multiple polymorphs with different space groups exist for a certain material, as for **5b**, one should carefully assess which polymorph is formed when constructing devices based on these compounds.

2.3.7 Dipole moments of the unit cell. Even though a polar space group is the first prerequisite for the application of the materials in the devices mentioned in the Introduction, it is ultimately the orientation of the molecular dipoles in the unit cell with respect to the polar axis of the crystal that determines the relevant properties of a candidate material. Zyss and Oudar theoretically derived the values of the optimal angles for maximum bulk quadratic (second-order) NLO behaviour between the dipolar axes of the molecules in the unit cell and the polar axis of the crystal, and found that for second-harmonic generation (SHG) these angles are 54.74° for the $P2_1$ space group (to which **5b-1** and **5c** belong) and 35.26° for Pc (to which **5e** belongs).³⁰ The graphical representations of the molecular dipoles as well as the unit cell dipoles, constituting the polar axes, of the crystal structures of **5b-1**, **5c** and **5e** are given in Fig. 10. Consistent with their space group symmetries, the unit cell dipoles are along the *b* axis for **5b-1** and **5c** in $P2_1$ and in the *ac* plane (the glide plane of the space group given in blue in Fig. 10c), making angles of about 31° and 59° with the $-a$ and *c* axes, respectively, for **5e** in Pc .

For **5b-1** (Fig. 10a), the net unit cell dipole amounts to 2.27 D and makes an angle of 79° with the two molecular dipoles. Comparison of the latter value with the theoretical value of 54.74° mentioned above suggests that **5b-1** will display bulk SHG to some extent. For **5e** (Fig. 10c), the sizeable unit cell dipole of 7.01 D makes an angle of about 66° with the two molecular dipoles. Comparison of this value with the angle of 35.26° given above leads to a similar conclusion as for **5b-1**. For **5c**, however, the two large molecular dipoles of the molecules in the unit cell are oriented in an *almost* completely

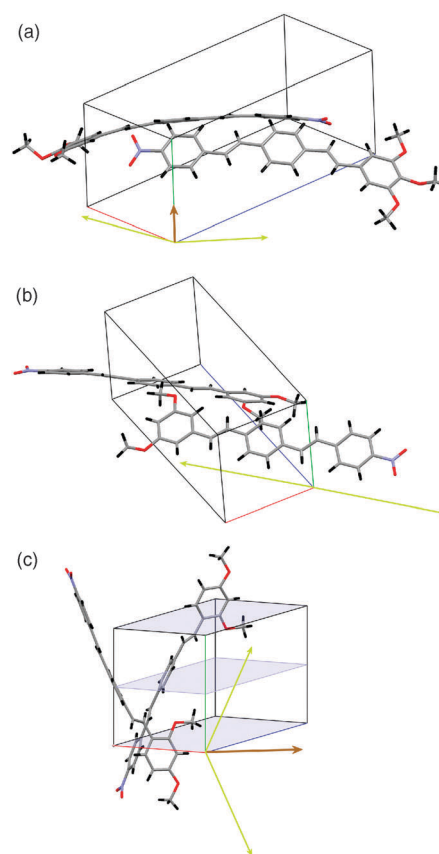


Fig. 10 Molecular dipoles of the individual molecules in the unit cell (green) and net dipole of the unit cell (brown) for the polar crystal structures of (a) **5b-1**, (b) **5c** and (c) **5e**.

anti-parallel fashion leading to a unit cell dipole of a mere 0.05 D—due to this limited size, it cannot actually be seen in Fig. 10b. Consequently, both molecular dipoles are virtually perpendicular to the unit cell dipole. This means that, even though **5c** crystallises in the non-centrosymmetric, polar space group $P2_1$ and must therefore have a non-zero macroscopic dipole, the latter's extremely limited size may preclude any useful properties, as the system must behave almost as a centrosymmetric one.

To put the properties of these new compounds into perspective, the size and orientation of the molecular and unit cell dipoles of 2-methyl-4-nitroaniline (MNA, CSD refcode BAJCIY02), a well-known SHG material,³¹ were analyzed in the same way. Each of the four molecules in the unit cell³² has a calculated molecular dipole of 7.93 D, leading to a sizeable unit cell dipole of 30.42 D. Consistent with its Cc space group, the unit cell dipole is found in the *ac* plane, making angles of about 19° and 109° with the $-a$ and *c* axes, respectively. Each of the four molecular dipoles makes an angle of about 16° with the unit cell dipole. Comparison of the latter value with the theoretically predicted one for that space group (35.26°) suggests a more efficient contribution of the molecular hyperpolarizability to the macroscopic one for MNA than for **5e**, for which the difference with the theoretical value is clearly larger. For a proper comparison of the NLO properties of these materials, though, the molecular hyperpolarizabilities of

the new compounds will have to be measured; these experiments are underway.

3. Conclusions

Twelve asymmetrical donor–acceptor distyrylbenzenes, containing one or more nitro or cyano groups as electron acceptors and one or more methoxy groups as electron donors, have been synthesized. The electronic properties were examined using CV, UV/Vis and quantum chemical calculations, and the effects of the substituents on these properties were described; although the reduction peak was absent from the voltammograms for all compounds, further experiments showed that the systems can be regarded as reversible and the anodic peak potentials were used as a measure for the oxidation potential. The solid-state structures of five of these new compounds were analyzed and described in function of the substitution pattern of the DSB scaffold: in general, the oligomers organise themselves in a head-to-tail fashion and generate CH \cdots O networks involving mainly the different methoxy groups. However, the compounds crystallize in both centrosymmetric and non-centrosymmetric, polar structures: in three of the six studied crystal structures the combined effects of the relatively weak intermolecular CH \cdots O and CH \cdots π interactions outweigh the otherwise dominating effects of the molecular dipoles and lead to non-centrosymmetric, polar structures. Analysis of the relative orientation of molecular and unit cell dipoles in the polar crystal structures leads to first insights into the NLO properties of these materials. Further experimental work to determine these properties is underway.

4. Experimental

4.1 Syntheses

All reagents and solvents were purchased from ACROS and used as received. ^1H and ^{13}C NMR spectra were recorded in CDCl_3 , unless stated otherwise, at 25 °C using a Bruker Avance II spectrometer operating at 400 MHz and 100 MHz, respectively; chemical shifts δ are given in ppm relative to tetramethylsilane (TMS) and coupling constants J are given in Hz. UV/Vis absorption spectra were recorded for solutions (about 20 μM) in CH_2Cl_2 on a Varian Cary 5 spectrophotometer.

4.1.1 Methylstilbenes (2b–d)

4.1.1.1 E-1-(4-Methylphenyl)-2-(3-nitrophenyl)ethene (2b). **2b** was prepared as is outlined in ref. 23. $\delta^1\text{H}$ 2.40 (s, 3H, CH_3), 7.08 (d, $^3J = 16.33$, 1H, H7), 7.21 (m, 3H, H8, H12 and H16), 7.44 (d, $^3J = 8.20$, 2H, H13 and H15), 7.51 (m, 1H, H5), 7.78 (dd, $^3J = 7.75$, $^4J = 1.01$, 1H, H6), 8.08 (ddd, $^3J = 8.17$, $^4J = 2.26$, $^4J = 1.01$, 1H, H4), 8.35 (dd, $^4J = 2.26$, $^4J = 1.01$, 1H, H2). $\delta^{13}\text{C}$ 21.3 (CH_3), 120.8 (C4), 121.8 (C2), 125.1 (C7), 126.8 (C13 and C15), 129.5 (C5), 129.6 (C12 and C16), 131.7 (C14), 132.1 (C6), 133.5 (C8), 138.6 (C1), 139.4 (C11), 148.8 (C3).

4.1.1.2 E-1-(4-Methylphenyl)-2-(2,4-dinitrophenyl)ethene (2c). A solution of sodium (2.3 g, 0.1 mol) in dry ethanol (80 ml) was added dropwise to a stirred mixture of **1** (40.3 g, 0.1 mol) and 2,4-dinitrobenzaldehyde (0.1 mol) in dry ethanol

(150 ml). The mixture was refluxed under a nitrogen atmosphere for 3 h. After cooling to room temperature, water (150 ml) was added to the reaction mixture and the precipitate was filtered off. The product was collected and redissolved in hot acetone (250 ml). This solution was poured into water (150 ml), after which the compound was collected by filtration. In order to obtain the pure *E* isomer, the compound was refluxed in *p*-xylene with a catalytic amount of iodine for 4 h. The yield was 33%. Mp 182 °C. $\delta^1\text{H}$ 2.40 (s, 3H, CH_3), 7.22 (d, $^3J = 8.24$, 2H, H12 and H16), 7.27 (d, $^3J = 16.17$, 1H, H7), 7.47 (d, $^3J = 8.24$, 2H, H13 and H15), 7.57 (d, $^3J = 16.17$, 1H, H8), 7.97 (d, $^3J = 8.70$, 1H, H6), 8.40 (dd, $^3J = 8.70$, $^4J = 2.29$, 1H, H5), 8.79 (d, $^4J = 2.29$, 1H, H3). $\delta^{13}\text{C}$ 21.4 (CH_3), 120.2 (C3), 120.7 (C7), 127.0 (C6), 127.6 (C13 and C15), 128.7 (C5), 129.8 (C12 and C16), 132.9 (C8), 138.2 (C14), 139.0 (C11), 140.3 (C1), 146.1 (C2), 147.4 (C4).

4.1.1.3 E-1-(4-Methylphenyl)-2-(4-cyanophenyl)ethene (2d).

2d was prepared as is outlined in ref. 18. $\delta^1\text{H}$ 2.37 (s, 3H, CH_3), 7.04 (d, $^3J = 16.33$, 1H, H7), 7.19 (m, 3H, H8, H12 and H16), 7.42 (d, $^3J = 8.24$, 2H, H13 and H15), 7.56 (d, $^3J = 8.69$, 2H, H2 and H6), 7.62 (d, $^3J = 8.54$, 2H, H3 and H5). $\delta^{13}\text{C}$ 21.3 (CH_3), 110.4 (C4), 119.0 (CN), 125.8 (C7), 126.7 (C3 and C5), 126.9 (C13 and C15), 129.6 (C12 and C16), 132.41 (C8), 132.44 (C2 and C6), 133.6 (C14), 138.8 (C11), 142.1 (C1).

4.1.2 Bromomethylstilbenes (3a–d)

4.1.2.1 E-1-(4-Bromomethylphenyl)-2-(4-nitrophenyl)ethene (3a). **3a** was prepared as is outlined in ref. 10. $\delta^1\text{H}$ 4.52 (s, 2H, CH_2), 7.15 (d, $^3J = 16.33$, 1H, H7), 7.25 (d, $^3J = 16.33$, 1H, H8), 7.42 (d, $^3J = 8.24$, 2H, H13 and H15), 7.52 (d, $^3J = 8.08$, 2H, H12 and H16), 7.63 (d, $^3J = 8.54$, 2H, H2 and H6), 8.23 (d, $^3J = 8.85$, 2H, H3 and H5). $\delta^{13}\text{C}$ 33.0 (CH_2), 124.2 (C12 and C16), 127.9 (C3 and C5), 127.0 (C7), 127.4 (C13 and C15), 129.6 (C2 and C6), 132.5 (C8), 136.4 (C14), 138.4 (C11), 143.57 (C1), 147.0 (C4).

4.1.2.2 E-1-(4-Bromomethylphenyl)-2-(3-nitrophenyl)ethene (3b). *N*-Bromosuccinimide (NBS) (7.1 g, 0.040 mol) and a catalytic amount of 1,1'-azobis(cyclohexanecarbonitrile) were added to a heated solution of **2b** (7.6 g, 0.032 mol) in CCl_4 (150 ml). The mixture was refluxed overnight. The hot solution was filtered to remove the succinimide. Then, the solvent was allowed to cool and partially evaporated. The precipitated product was collected by filtration. The yield was 47%. Mp 107 °C. $\delta^1\text{H}$ 4.51 (s, 2H, CH_2), 7.13 (d, $^3J = 16.33$, 1H, H7), 7.22 (d, $^3J = 16.33$, 1H, H8), 7.40–7.60 (m, 5H, H5, H12, H13, H15, H16), 7.79 (dd, $^3J = 7.76$, $^4J = 1.12$, 1H, H6), 8.10 (ddd, $^3J = 7.88$, $^4J = 2.20$, $^4J = 1.12$, 1H, H4), 8.36 (d, $^4J = 2.20$, 1H, H2). $\delta^{13}\text{C}$ 33.14 (CH_2), 120.97 (C4), 122.22 (C2), 126.88 (C7), 127.22 (C12 and C16), 129.91 (C13 and C15), 129.68 (C14), 130.99 (C6), 132.31 (C8), 136.51 (C11), 138.04 (C1), 138.96 (C11), 148.81 (C3).

4.1.2.3 E-1-(4-Bromomethylphenyl)-2-(2,4-dinitrophenyl)ethene (3c). **3c** was prepared as is outlined in ref. 24. $\delta^1\text{H}$ 4.52 (s, 2H, CH_2), 7.26 (d, $^3J = 16.17$, 1H, H7), 7.45 (d, $^3J = 8.24$, 2H, H13 and H15), 7.55 (d, $^3J = 8.24$, 2H, H12 and H16), 7.66 (d, $^3J = 16.18$, 2H, H8), 7.98 (d, $^3J = 8.70$, 1H, H6), 8.43 (dd, $^3J = 8.70$, $^4J = 2.29$, 1H, H5), 8.83 (d, $^4J = 2.29$, 1H, H3).

Due to the limited solubility of **3c** no ^{13}C NMR spectrum of sufficient quality could be obtained.

4.1.2.4 E-1-(4-Bromomethylphenyl)-2-(4-cyanophenyl)ethene (3d). **3d** was prepared as is outlined in ref. 18. $\delta^1\text{H}$ 4.51 (s, 2H, CH_2), 7.09 (d, $^3J = 16.33$, 1H, H7), 7.19 (d, $^3J = 16.33$, 1H, H8), 7.41 (d, $^3J = 8.24$, 2H, H13 and H15), 7.50 (d, $^3J = 8.24$, 2H, H12 and H16), 7.58 (d, $^3J = 8.39$, 2H, H3 and H5), 7.63 (d, $^3J = 8.55$, 2H, H2 and H6). $\delta^{13}\text{C}$ 33.1 (CH_2), 110.9 (C4), 118.9 (CN), 126.9 (C2 and C6), 127.3 (C12 and C16), 127.5 (C7), 129.6 (C13 and C15), 131.6 (C8), 132.5 (C3 and C5), 136.6 (C14), 138.1 (C11), 141.6 (C1).

4.1.3 Phosphonium salts (4b–c)

4.1.3.1 E-Triphenyl[4-(2-(3-nitrophenyl)ethenyl)benzyl]-phosphonium bromide (4b). Triphenylphosphine (6.6 g, 0.025 mol) was added to a solution of **3b** (7.3 g, 0.023 mol) in acetonitrile (150 ml). The solution was refluxed for 4 h. After cooling to room temperature, the product was collected by filtration and washed with diethyl ether. The yield was 76%. Mp > 250 °C (decomp.).

4.1.3.2 E-Triphenyl[4-(2-(2,4-dinitrophenyl)ethenyl)benzyl]-phosphonium bromide (4c). Triphenylphosphine (6.6 g, 0.025 mol) was added to a solution of **3c** (8.3 g, 0.023 mol) in acetonitrile (150 ml). The solution was refluxed for 4 h. After cooling to room temperature, the product was collected by filtration and washed with diethyl ether. The yield was 39%. Mp 255 °C (decomp.).

4.1.4 Oligomers 5b–k. In the general procedure, sodium (0.4 g, 16.5 mmol) in dry ethanol (40 ml) was added dropwise to a stirred mixture of the appropriate phosphonium salt **4a–d** (16.5 mmol) and the appropriate methoxybenzaldehyde (16.5 mmol) in dry ethanol (100 ml). The mixture was refluxed under a nitrogen atmosphere for 6 h. After cooling to room temperature, water (125 ml) was added. The mixture was filtered and the product washed with diethyl ether. To obtain the pure *E,E* isomer, the product was refluxed in *p*-xylene with a catalytic amount of iodine for 4 h. After cooling, the product was collected by filtration. NMR spectroscopic data of **5a** can be found in ref. 10.

4.1.4.1 E,E-1-[2-(4-Nitrophenyl)ethenyl]-4-[2-(3,4,5-trimethoxyphenyl)ethenyl]benzene (5b). Yield 14%. Mp 180 °C [for the red polymorph (**5b-1**); the yellow polymorph (**5b-2**) transforms into the red upon heating]. $\delta^1\text{H}$ 3.88 (s, 3H, H40), 3.93 (s, 6H, H30 and H50), 6.76 (s, 2H, C22 and C26), 7.02 (d, $^3J = 16.22$, 1H, H18), 7.10 (d, $^3J = 16.22$, 1H, H17), 7.16 (d, $^3J = 16.31$, 1H, H7), 7.27 (d, $^3J = 16.31$, 1H, H8), 7.51–7.58 (m, 4H, H12, H13, H15 and H16), 7.64 (d, $^3J = 8.59$, 2H, H2 and H6), 8.22 (d, $^3J = 8.59$, 2H, H3 and H5). $\delta^{13}\text{C}$ 56.21 (C30 and C50), 60.99 (C40), 103.87 (C22 and C26), 124.19 (C3 and C5), 126.10 (C7), 126.83 (C2 and C6), 126.92 (C13 and C15), 127.47 (C12 and C16), 129.43 (C8), 132.86 (C18), 135.47 (C14), 137.9 (C21), 138.40 (C24), 143.90 (C1), 146.79 (C4), 153.52 (C23 and C25).

4.1.4.2 E,E-1-[2-(4-Nitrophenyl)ethenyl]-4-[2-(3,5-dimethoxyphenyl)ethenyl]benzene (5c). Yield 85%. Mp 172 °C. $\delta^1\text{H}$ 3.84 (s, 6H, H30 and H50), 6.42 (t, $^4J = 2.25$, 1H, H24), 6.68 (d, $^4J = 2.25$, 2H, H22 and H26), 7.08 (m, 2H, H17 and H18), 7.15 (d, $^3J = 16.31$, 1H, H7), 7.25 (d, $^3J = 16.30$, 1H, H8), 7.48–7.58

(m, 4H, H12, H13, H15, H16), 7.62 (d, $^3J = 8.86$, 2H, H2 and H6), 8.21 (d, $^3J = 8.86$, 2H, H3 and H5). $\delta^{13}\text{C}$ 55.4 (C30 and C50), 100.3 (C24), 104.8 (C22 and C26), 124.2 (C3 and C5), 126.2 (C7), 126.8 (C2 and C6), 127.1 (C13 and C15), 127.4 (C12 and C16), 128.5 (C17), 129.5 (C8), 132.9 (C18), 135.6 (C14), 137.8 (C21), 139.2 (C11), 143.9 (C1), 146.8 (C4), 161.1 (C23 and C25).

4.1.4.3 E,E-1-[2-(4-Nitrophenyl)ethenyl]-4-[2-(2,6-dimethoxyphenyl)ethenyl]benzene (5d). Yield 59%. Mp 151 °C. $\delta^1\text{H}$ (MeOD) 3.89 (s, 6H, H20 and H60), 6.58 (d, $^3J = 8.32$, 2H, H23 and H25), 7.08 (d, $^3J = 16.33$, 1H, H7), 7.14–7.23 (m, 2H, H8 and H24), 7.47–7.58 (m, 8H, H2, H6, H12, H13, H15, H16, H17 and H18), 8.17 (d, $^3J = 8.31$, 2H, H3 and H5). $\delta^{13}\text{C}$ (MeOD) 55.83 (C20 and C60), 104.07 (C23 and C25), 114.68 (C21), 120.82 (C17), 124.11 (C3 and C5), 125.47 (C7), 126.72 (C2 and C5), 126.86 (C13 and C15), 127.29 (C12 and C16), 128.44 (C8), 131.55 (C24), 133.20 (C18), 134.76 (C14), 140.15 (C11), 144.09 (C1), 146.59 (C4), 158.78 (C22 and C26).

4.1.4.4 E,E-1-[2-(4-Nitrophenyl)ethenyl]-4-[2-(2,4-dimethoxyphenyl)ethenyl]benzene (5e). **5e** was prepared as is outlined in ref. 24. Yield 44%. Mp 172 °C. $\delta^1\text{H}$ 3.84 (s, 3H, H40), 3.89 (s, 3H, H20), 6.48 (d, $^4J = 2.40$, 1H, H23), 6.53 (dd, $^3J = 8.44$, $^4J = 2.40$, 1H, H25), 7.02 (d, $^3J = 16.43$, 1H, H7), 7.13 (d, $^3J = 16.43$, 1H, H8), 7.26 (d, $^3J = 8.44$, 1H, H26), 7.26 (d, $^3J = 16.31$, 1H, H17), 7.45 (d, $^3J = 16.47$, 1H, H18), 7.51 (d, $^3J = 9.02$, 2H, H13 and H15), 7.54 (d, $^3J = 9.06$, 2H, H12 and H16), 7.63 (d, $^3J = 8.88$, 2H, H2 and H6), 8.22 (d, $^3J = 8.88$, 2H, H3 and H5). $\delta^{13}\text{C}$ 55.45 (C40), 55.57 (C20), 98.57 (C23), 105.19 (C25), 119.36 (C21), 124.17 (C3 and C5), 125.58 (C7), 126.24 (C26), 126.76 (C2 and C6), 127.30 (C17), 127.37 (C13 and C15), 127.38 (C12 and C16), 130.26 (C8), 133.14 (C18), 137.77 (C14), 139.13 (C11), 144.08 (C1), 146.66 (C4), 158.23 (C22), 160.84 (C24).

4.1.4.5 E,E-1-[2-(4-Nitrophenyl)ethenyl]-4-[2-(4-methoxyphenyl)ethenyl]benzene (5f). **5f** was prepared as is outlined in ref. 24. Yield 60%. Mp 251 °C. $\delta^1\text{H}$ 3.84 (s, 3H, H40), 6.91 (d, $^3J = 8.80$, 2H, H23 and H25), 6.98 (d, $^3J = 16.31$, 1H, H7), 7.12 (d, $^3J = 16.31$, 1H, H8), 7.14 (d, $^3J = 16.27$, 1H, H17), 7.26 (d, $^3J = 16.27$, 1H, H18), 7.47 (d, $^3J = 8.56$, 2H, H22 and H26), 7.51 (d, $^3J = 8.93$, 2H, H12 and H16), 7.54 (d, $^3J = 8.93$, 2H, H13 and H15), 7.63 (d, $^3J = 8.64$, 2H, H2 and H6), 8.22 (d, $^3J = 8.83$, 2H, H3 and H5). $\delta^{13}\text{C}$ 55.37 (C40), 114.27 (C23 and C25), 124.20 (C3 and C5), 125.84 (C7), 125.91 (C17), 126.74 (C12 and C16), 126.80 (C2 and C6), 127.44 (C22 and C26), 127.88 (C13 and C15), 129.98 (C21), 129.99 (C8), 133.02 (C18), 135.08 (C11), 138.42 (C14), 144.00 (C1), 146.76 (C4), 159.61 (C24).

4.1.4.6 E,E-1-[2-(3-Nitrophenyl)ethenyl]-4-[2-(2,4,6-trimethoxyphenyl)ethenyl]benzene (5g). Yield 42%. Mp 176 °C. $\delta^1\text{H}$ 3.85 (s, 3H, H40), 3.90 (s, 6H, H20 and H60), 6.18 (s, 2H, H23 and H25), 7.11 (d, $^3J = 16.30$, 1H, H7), 7.22 (d, $^3J = 16.30$, 1H, H8), 7.45–7.60 (m, 7H, H3, H12, H13, H15, H16, H17 and H18), 7.79 (dd, $^3J = 7.70$, $^4J = 1.0$, 1H, H6), 8.07 (ddd, $^3J = 8.20$, $^4J = 2.20$, $^4J = 1.0$, 1H, H4), 8.36 (d, $^4J = 2.20$, 1H, H2). $\delta^{13}\text{C}$ 55.3 (C40), 55.8 (C20 and C60), 90.9 (C23 and C25), 108.2 (C21), 120.6 (C4), 120.8 (C17), 121.8 (C2), 125.1 (C7), 126.6 (C13 and C15), 127.1 (C12 and C16), 129.2

and 129.5 (C5 and C8), 131.8 and 132.1 (C6 and C18), 134.4 (C14), 139.5 (C1), 140.3 (C11), 148.8 (C3), 159.7 (C23 and C25), 160.5 (C24).

4.1.4.7 E,E-1-[2-(2,4-Dinitrophenyl)ethenyl]-4-[2-(2,4,6-trimethoxyphenyl)ethenyl]benzene (5h). **5h** was prepared as is outlined in ref. 24. Yield 33%. Mp 210 °C. $\delta^1\text{H}$ 3.85 (s, 3H, H40), 3.90 (s, 6H, H20 and H60), 6.18 (s, 2H, H23 and H25), 7.29 (d, $^3J = 16.07$, 1H, H8), 7.51 (m, 6H, H12, H13, H15, H16, H17 and H18), 7.62 (d, $^3J = 16.07$, 1H, H7), 7.98 (d, $^3J = 8.80$, 1H, H6), 8.40 (dd, $^3J = 8.80$, $^4J = 2.38$, 1H, H5), 8.80 (d, $^4J = 2.34$, 1H, H3). $\delta^{13}\text{C}$ 55.37 (C40), 55.83 (C20 and C60), 90.89 (C23 and C25), 107.98 (C21), 119.82 (C3), 120.82 (C17), 126.7 (C7), 126.92 (C5), 127.98 (C13 and C15), 128.79 (C6), 128.92 (C12 and C16), 133.60 (C8), 134.69 (C18), 138.3 (C14), 139.05 (C11), 141.79 (C1), 145.92 (C4), 147.29 (C2), 159.80 (C22 and C26), 160.75 (C24).

4.1.4.8 E,E-1-[2-(4-Cyanophenyl)ethenyl]-4-[2-(2,4,6-trimethoxyphenyl)ethenyl]benzene (5i). Yield 40%. Mp 196 °C. $\delta^1\text{H}$ 3.85 (s, 3H, H40), 3.90 (s, 6H, H20 and H60), 6.18 (s, 2H, H23 and H25), 7.06 (d, $^3J = 16.33$, 1H, H7), 7.20 (d, $^3J = 16.33$, 1H, H8), 7.46 (m, 2H, H17 and H18), 7.48 (d, $^3J = 8.54$, 2H, H13 and H15), 7.52 (d, $^3J = 8.55$, 2H, H12 and H16), 7.56 (d, $^3J = 8.39$, 2H, H2 and H6), 7.62 (d, $^3J = 8.39$, 2H, H3 and H5). $\delta^{13}\text{C}$ 55.4 (C40), 55.8 (C20 and C60), 91.0 (C23 and C25), 108.2 (C21), 110.3 (C4), 119.1 (CN), 120.7 (C17), 125.7 (C7), 126.6 (C12 and C16), 126.7 (C2 and C6), 127.1 (C13 and C15), 129.2 (C18), 132.4 (C3 and C5), 134.4 (C14), 140.4 (C11), 142.2 (C1), 159.7 (C22 and C26), 160.5 (C24).

4.1.4.9 E,E-1-[2-(4-Cyanophenyl)ethenyl]-4-[2-(2,4-dimethoxyphenyl)ethenyl]benzene (5j). Yield 38%. Mp 162 °C. $\delta^1\text{H}$ 3.84 (s, 3H, H40), 3.88 (s, 3H, H20), 6.48 (s, 1H, H23), 6.51 (d, $^3J = 8.24$, 1H, H25), 7.01 (d, $^3J = 16.33$, 1H, H7), 7.19 (d, $^3J = 16.32$, 1H, H8), 7.38 (d, $^3J = 16.32$, 1H, H17), 7.41 (d, $^3J = 16.32$, 1H, H18), 7.49 (d, $^3J = 8.49$, 2H, H13 and H15), 7.52 (d, $^3J = 8.64$, 2H, H12 and H16), 7.53 (d, $^3J = 8.59$, 1H, H26), 7.56 (d, $^3J = 8.35$, 2H, H2 and H6). Due to the limited solubility of **5j** no ^{13}C NMR spectrum of sufficient quality could be obtained.

4.1.4.10 E,E-1-[2-(4-Cyanophenyl)ethenyl]-4-[2-(4-methoxyphenyl)ethenyl]benzene (5k). Yield 39%. Mp 245 °C. $\delta^1\text{H}$ 3.84 (s, 3H, H40), 6.55 (d, $^3J = 8.60$, 2H, H23 and H25), 6.97 (d, $^3J = 16.19$, 1H, H7), 7.08 (d, $^3J = 16.19$, 1H, H8), 7.11 (d, $^3J = 16.31$, 1H, H17), 7.21 (d, $^3J = 16.31$, 1H, H18), 7.49 (d, $^3J = 8.60$, 2H, H22 and H26), 7.51 (m, 4H, H12, H13, H15 and H16), 7.58 (d, $^3J = 8.24$, 2H, H2 and H6), 7.63 (d, $^3J = 8.24$, 2H, H3 and H5). Due to the limited solubility of **5k** no ^{13}C NMR spectrum of sufficient quality could be obtained.

4.1.5 Oligomer 5l

4.1.5.1 E-Triphenyl[4-(2-(2,4,6-trimethoxyphenyl)ethenyl)-benzyl]phosphonium bromide (8). A solution of sodium ethanolate in dry ethanol, prepared by reacting sodium (0.6 g, 0.025 mol) with dry ethanol (50 ml), was added dropwise to a mixture of 1,4-bis(triphenylphosphonium-methyl)-benzene dibromide (39.4 g, 0.050 mol) and of 2,4,6-trimethoxybenzaldehyde (6.0 g, 0.025 mol) in dry ethanol (200 ml) under a nitrogen atmosphere. The solution was stirred

overnight. Subsequently, water (300 ml) was added, after which the main by-product (*i.e.*, the symmetric distyrylbenzene) was filtered off. The solvent was evaporated and the residue was redissolved in DMF. The remaining precipitate (*i.e.*, the bisphosphonium starting product) was filtered off and the solution was placed in the refrigerator overnight. The precipitate was again filtered off and the solvent was evaporated. Toluene (200 ml) was added to the residue and the resulting precipitate was the desired compound, which was washed with ether and dried in air. The yield was 35%. Mp > 250 °C.

4.1.5.2 E,E-1-[2-(2,4,6-Trinitrophenyl)ethenyl]-4-[2-(2,4,6-trimethoxyphenyl)ethenyl]benzene (5l). Sodium (0.08 g, 3.3 mmol) in dry ethanol (30 ml) was added dropwise to a stirred mixture of **7** (0.75 g, 3.3 mmol) and **8** (2.1 g, 3.3 mol) in dry ethanol (60 ml). The mixture was refluxed under nitrogen atmosphere for 6 h. After cooling to room temperature, the mixture was filtered and the dark red product washed with diethyl ether. To obtain the pure *E* isomer, the product was refluxed in *p*-xylene with a catalytic amount of iodine for 4 h. After cooling, the product was collected by filtration. Yield 25%. Mp 200 °C. $\delta^1\text{H}$ (MeOD) 3.81 (s, 3H, H40), 3.85 (s, 6H, H20 and H60), 6.22 (s, 2H, H23 and H25), 7.50–7.90 (m, 8H, H7, H8, H12, H13, H15, H16, H17, H18), 8.54 (s, 2H, H5 and H3). Due to the limited solubility of **5l** no ^{13}C NMR spectrum of sufficient quality could be obtained.

4.2 X-Ray diffraction

For all compounds, attempts were made to grow suitable crystals *via* diffusion, slow evaporation and slow cooling, using various solvents. Both polymorphs of **5b** and **5i** were obtained from a CH_2Cl_2 solution and **5c** crystallized by slow evaporation of a THF solution. The collection of diffraction data of sufficient quality was performed on an Enraf-Nonius Mach 3 diffractometer with single-point detector using Mo-K α radiation ($\lambda = 0.71073 \text{ \AA}$) for compounds **5b** (two polymorphs, **5b-1** and **5b-2**), **5c** and **5i**, although the crystals of **5b-2** and **5i** were relatively weakly diffracting and produced data of somewhat lower quality. Details on the crystallization and data collection of **5a**¹⁰ and **5e**²⁷ can be found elsewhere. For the non-centrosymmetric structures **5b-1** and **5c**, the Friedel pairs were collected independently, but were merged in the final refinement; due to the fact that there are no anomalous scatterers (atoms with $Z > Z_{\text{Si}}$) an absolute structure could not be determined and it was chosen arbitrarily.

The structures of **5b-1**, **5c** and **5i** showed disorder consisting of a 180° twist of one of the ethenylic links. The model used in the variable-temperature study of the disorder in **5c** is reported elsewhere:²⁷ in it the disorder has been described taking into account the complete stilbene fragment, *i.e.*, the two rings and the spacer. For compound **5b-1**, however, such a complete model could not be used, in part due to the limited size of the crystal. Incorporation of the complete peripheral ring (with or without all of the methoxy groups) into the model led to convergence problems (even with 500 LS-cycles) due to the large number of restraints, or meaningless geometrical and anisotropic displacement parameters, as did the inclusion of only parts of the rings. Ultimately, assuming a dynamic pedal motion (see ref. 27 and references therein), the ethenylic spacer

was treated as a rigid group. The C17–C18 and C17B–C18B distances were restrained to be similar (SADI) and the C14–C17 and C21–C18 distances were restrained to 1.45 Å (DFIX). The atoms of the pairs C12/C13, C15/C16, C17/C17B and C18/C18B were constrained to possess identical ADPs (EADP). The atoms of the pairs C25/C26 and C22/C23 were restrained to possess similar ADPs (SIMU). For compound **5i**, a similar model was used. The C7–C8 and C7B–C8B, C21–C8 and C21–C8B, and C4–C7 and C4–C7B distances were restrained to be similar (SADI). The atoms of the pairs C7/C7B and C8/C8B were constrained to possess identical ADPs (EADP). The generation of “anti-bumping” restraints also proved to be necessary (BUMP).

Hydrogen atoms were placed in calculated positions and refined as riding with C–H distances of 0.93 Å. For the analysis of the supramolecular structures, the C–H bond lengths were normalized to the value derived from neutron diffraction (1.083 Å).³³ The CAD-4 EXPRESS³⁴ software was used for data collection and cell refinement and XCAD-4³⁵ for data reduction. The structures were solved by direct methods using SHELXS-97³⁶ and refined using SHELXL-97.³⁶ WinGX (version 1.80)³⁷ and PLATON³⁸ were used to prepare the material for publication and figures were drawn using ORTEP3³⁹ for Windows and MERCURY (version 2.2).⁴⁰ The experimental details including the results of the refinements are given in Table 2. The numbering scheme can be found in Fig. 1. CCDC 760975 (**5b-1**), 760976 (**5b-2**), 760977 (**5c**) and 760979 (**5i**) contain the supplementary crystallographic data for this paper.

4.3 Quantum chemical calculations

Quantum chemical calculations were performed using the Gaussian 03⁴¹ suite of programs at the DFT/B3LYP/6-31G* level of theory; the basis set was used as it is implemented in the program. Optimized geometries were calculated in C_1 (for **5b**, **5h** and **5l**) or C_s (for **5a**, **5c**, **5d**, **5e**, **5f**, **5g**, **5i**, **5j** and **5k**) symmetry. Frequency calculations were performed to verify that the resulting structures are energy minima. Ionization Potentials (IP) were calculated using Koopmans' theorem.⁴² Molecular dipoles of the two molecules in the unit cells of **5b-1**, **5c** and **5e** were calculated in their solid-state geometries (for **5b-1** and **5e**, only the major conformer was considered) at the same level of theory; these values are also given in Table 1. The resulting vectors were then transformed from the Cartesian to the unit cell coordinate system.

4.4 Electrochemical measurements

Electrochemical measurements were performed using an AUTOLAB potentiostat/galvanostat connected to a PC equipped with the “General Purpose Electrochemical System” (GPES) software. Cyclic voltammetric (CV) measurements were carried out in dry acetonitrile at 298 K under an argon atmosphere. Tetrabutylammonium tetrafluoroborate obtained from ALDRICH was used as the supporting electrolyte. Concentrations of 0.4 mM and 80 mM for the oligomer and electrolyte, respectively, were used, except for compound **5f**, for which a solution of only 0.2 mM of oligomer was used, due to its limited solubility; the solubility of **5l** proved to be too

low to allow any measurement. Extra dry acetonitrile (<50 ppm water) was purchased from ACROS and stored on 3 Å sieves. Standard voltammograms were recorded at a scan rate of 0.1 V s⁻¹, while measurements to ascertain the reversibility of the systems were performed at scan rates of 0.03, 0.05, 0.1, 0.25 and 1 V s⁻¹; the ferrocene/ferrocenium (Fc/Fc⁺) couple was used as a reference.⁴³ The working electrode was a BASi stationary voltammetry electrode comprising a platinum electrode disc with a diameter of 3 mm. A platinum plate was used as the auxiliary electrode and a silver wire as the pseudo-reference electrode.

Acknowledgements

A. C. and R. D. B. wish to thank the Institute for the Promotion of Innovation through Science and Technology in Flanders (IWT-Vlaanderen) for a research grant. C. V. V. wishes to thank the Fund for Scientific Research (FWO Vlaanderen) for a grant as a research assistant. Financial support by FWO-Vlaanderen under grant G.0129.05 and by the University of Antwerp under Grant GOA-2404 is gratefully acknowledged. The authors gratefully acknowledge the University of Antwerp for access to the university's computer cluster CalcUA.

References

- 1 K. Müllen and G. Wegner, *Electronic Materials—The Oligomer Approach*, Wiley-VCH, Weinheim, 1998.
- 2 J. L. Segura and N. Martin, *J. Mater. Chem.*, 2000, **10**, 2403–2435.
- 3 M. Hakansson, S. Jagner, M. Sundahl and O. Wennerstrom, *Acta Chem. Scand.*, 1992, **46**, 1160–1165.
- 4 H. Irngartinger, J. Lichtenthaler and R. Herpich, *Struct. Chem.*, 1994, **5**, 283–289.
- 5 J. K. Baeke, J. Nowaczyk, M. Moens, L. J. Chen, P. Dieltiens, H. J. Geise, C. Van Alsenoy and F. Blockhuys, *J. Electroanal. Chem.*, 2007, **599**, 1–11.
- 6 C. M. L. Vande Velde, J. K. Baeke, H. J. Geise and F. Blockhuys, *Acta Crystallogr., Sect. C: Cryst. Struct. Commun.*, 2005, **61**, o284–o287.
- 7 C. M. L. Vande Velde, L. J. Chen, J. K. Baeke, M. Moens, P. Dieltiens, H. J. Geise, M. Zeller, A. D. Hunter and F. Blockhuys, *Cryst. Growth Des.*, 2004, **4**, 823–830.
- 8 C. M. L. Vande Velde, H. J. Geise and F. Blockhuys, *Acta Crystallogr., Sect. C: Cryst. Struct. Commun.*, 2005, **61**, o21–o24.
- 9 C. M. L. Vande Velde, H. J. Geise and F. Blockhuys, *Cryst. Growth Des.*, 2006, **6**, 241–246.
- 10 C. M. L. Vande Velde, R. De Borger and F. Blockhuys, *Acta Crystallogr., Sect. E: Struct. Rep. Online*, 2005, **61**, o4289–o4291.
- 11 G. P. Bartholomew, X. H. Bu and G. C. Bazan, *Chem. Mater.*, 2000, **12**, 1422–1430.
- 12 G. P. Bartholomew, X. H. Bu and G. C. Bazan, *Chem. Mater.*, 2000, **12**, 2311–2318.
- 13 G. W. Coates, A. R. Dunn, L. M. Henling, J. W. Ziller, E. B. Lobkovsky and R. H. Grubbs, *J. Am. Chem. Soc.*, 1998, **120**, 3641–3649.
- 14 B. Nohra, S. Graule, C. Lescop and R. Reau, *J. Am. Chem. Soc.*, 2006, **128**, 3520–3521.
- 15 M. L. Renak, G. P. Bartholomew, S. J. Wang, P. J. Ricatto, R. J. Lachicotte and G. C. Bazan, *J. Am. Chem. Soc.*, 1999, **121**, 7787–7799.
- 16 J. C. Sancho-Garcia, J.-L. Brédas, D. Beljonne, J. Cornil, R. Martínez-Alvarez, M. Hanack, L. Poulsen, J. Gierschner, H.-G. Mack, H.-J. Egelhaaf and G. Oelkrug, *J. Phys. Chem. B*, 2005, **109**, 4872–4880.
- 17 M. Zeller, A. D. Hunter, R. Hoefnagels, H. J. Geise and F. Blockhuys, *Acta Crystallogr., Sect. E: Struct. Rep. Online*, 2005, **61**, o4183–o4184.

- 18 R. Ercel and H. Fruhbais, *Z. Naturforsch., B: Chem. Sci.*, 1982, **37**, 1472–1480.
- 19 J. K. Baekke, R. De Borger, F. Lemièrre, C. Van Alsenoy and F. Blockhuys, *J. Phys. Org. Chem.*, 2009, **22**, 925–932.
- 20 F. H. Allen, *Acta Crystallogr., Sect. B: Struct. Sci.*, 2002, **58**, 380–388.
- 21 D. N. Nicolaides, K. E. Litinas, G. K. Papageorgiou and J. Stephanidoustephanatou, *J. Heterocycl. Chem.*, 1991, **28**, 139–143.
- 22 R. De Borger, C. M. L. Vande Velde and F. Blockhuys, *Acta Crystallogr., Sect. E: Struct. Rep. Online*, 2005, **61**, o819–o821.
- 23 P. L'Ecuyer, F. Turcotte, J. Giguere, C. A. Olivier and P. Roberge, *Can. J. Res., Sect. B*, 1948, **26**, 70–80.
- 24 G. Manecke and S. Luettker, *Chem. Ber.*, 1970, **103**, 700–707.
- 25 S. Secareanu, *Chem. Ber.*, 1931, **64**, 834–841.
- 26 M. Kroger and G. Fels, *J. Labelled Compd. Radiopharm.*, 2000, **43**, 217–227.
- 27 C. M. L. Vande Velde, A. Collas, R. De Borger and F. Blockhuys, *Chem.–Eur. J.*, DOI: 10.1002/chem.201002472, in press.
- 28 Y. H. Liu, T. L. Zhang, J. G. Zhang, L. Yang, J. Y. Guo, W. Yu, R. F. Wu and K. B. Yu, *Can. J. Chem.*, 2006, **84**, 867–873.
- 29 W. J. Feast, P. W. Lovenich, H. Puschmann and C. Taliani, *Chem. Commun.*, 2001, 505–506.
- 30 J. Zyss and J. L. Oudar, *Phys. Rev. A: At., Mol., Opt. Phys.*, 1982, **26**, 2028–2048.
- 31 B. F. Levine, C. G. Bethea, C. D. Thurmond, R. T. Lynch and J. L. Bernstein, *J. Appl. Phys.*, 1979, **50**, 2523–2527.
- 32 G. F. Lipscomb, A. F. Garito and R. S. Narang, *J. Chem. Phys.*, 1981, **75**, 1509–1515.
- 33 F. H. Allen, O. Kennard, D. G. Watson, L. Brammer, A. G. Orpen and R. Taylor, *J. Chem. Soc., Perkin Trans. 2*, 1987, S1–S19.
- 34 Enraf-Nonius, *CAD-4 EXPRESS*, 1994, Delft, The Netherlands.
- 35 K. Harms and S. Wocadlo, *XCAD4*, University of Marburg, Germany, 1996.
- 36 G. M. Sheldrick, *Acta Crystallogr., Sect. A: Found. Crystallogr.*, 2008, **64**, 112–122.
- 37 L. J. Farrugia, *J. Appl. Crystallogr.*, 1999, **32**, 837–838.
- 38 A. L. Spek, *J. Appl. Crystallogr.*, 2003, **36**, 7–13.
- 39 L. J. Farrugia, *J. Appl. Crystallogr.*, 1997, **30**, 565.
- 40 C. F. Macrae, I. J. Bruno, J. A. Chisholm, P. R. Edgington, P. McCabe, E. Pidcock, L. Rodriguez-Monge, R. Taylor, J. van de Streek and P. A. Wood, *J. Appl. Crystallogr.*, 2008, **41**, 466–470.
- 41 M. J. Frisch, G. W. Trucks, H. B. Schlegel, G. E. Scuseria, M. A. Robb, J. R. Cheeseman, J. A. J. Montgomery, T. Vreven, K. N. Kudin, J. C. Burant, J. M. Millam, S. S. Iyengar, J. Tomasi, V. Barone, B. Mennucci, M. Cossi, G. Scalmani, N. Rega, G. A. Petersson, H. Nakatsuji, M. Hada, M. Ehara, K. Toyota, R. Fukuda, J. Hasegawa, M. Ishida, T. Nakajima, Y. Honda, O. Kitao, H. Nakai, M. Klene, X. Li, J. E. Knox, H. P. Hratchian, J. B. Cross, C. Adamo, J. Jaramillo, R. Gomperts, R. E. Stratmann, O. Yazyev, A. J. Austin, R. Cammi, C. Pomelli, J. W. Ochterski, P. Y. Ayala, K. Morokuma, G. A. Voth, P. Salvador, J. J. Dannenberg, V. G. Zakrzewski, S. Dapprich, A. D. Daniels, M. C. Strain, O. Farkas, D. K. Malick, A. D. Rabuck, K. Raghavachari, J. B. Foresman, J. V. Ortiz, Q. Cui, A. G. Baboul, S. Clifford, J. Cioslowski, B. B. Stefanov, A. L. G. Liu, P. Piskorz, I. Komaromi, R. L. Martin, D. J. Fox, T. Keith, M. A. Al-Laham, C. Y. Peng, A. Nanayakkara, M. Challacombe, P. M. W. Gil, B. Johnson, W. Chen, M. W. Wong, C. Gonzalez and J. A. Pople, *Gaussian 03*, Gaussian Inc., Pittsburg, PA, 2003.
- 42 T. Koopmans, *Physica*, 1934, **1**, 104.
- 43 G. Gritzner and J. Kuta, *Pure Appl. Chem.*, 1984, **56**, 461–466.